Magnetic susceptibility of $YbRh_2Si_2$ and $YbIr_2Si_2$ on the basis of a localized 4f electron approach

2008 J. Phys.: Condens. Matter 20 455208

(http://iopscience.iop.org/0953-8984/20/45/455208)

J. Phys.: Condens. Matter **20** (2008) 455208 (6pp) doi:10.1088/0953-8984/20/45/455208

Magnetic susceptibility of $YbRh_2Si_2$ and $YbIr_2Si_2$ on the basis of a localized 4f electron approach

A S Kutuzov[1], A M Skvortsova[1], S I Belov[1], J Sichelschmidt[2], J Wykhoff[2], I Eremin[3], C Krellner[2], C Geibel[2] and B I Kochelaev[1]

[1] Physics Department, Kazan State University, 420008 Kazan, Russia
[2] Max Planck Institute for Chemical Physics of Solids, D-01187 Dresden, Germany
[3] Max Planck Institute for the Physics of Complex Systems, D-01187 Dresden, Germany

E-mail: Sichelschmidt@cpfs.mpg.de

Received 31 July 2008, in final form 10 September 2008
Published 13 October 2008
Online at stacks.iop.org/JPhysCM/20/455208

Abstract

We consider the local properties of the Yb^{3+} ion in the crystal electric field in the Kondo lattice compounds $YbRh_2Si_2$ and $YbIr_2Si_2$. On this basis we have calculated the magnetic susceptibility, taking into account the Kondo interaction in the simplest molecular field approximation. The resulting Curie–Weiss law and Van Vleck susceptibilities could be excellently fitted to experimental results over a wide temperature interval where thermodynamic and transport properties show non-Fermi-liquid behavior for these materials.

(Some figures in this article are in colour only in the electronic version)

1. Introduction

Very peculiar magnetic, thermal and transport properties of 4f-electron-based heavy fermion systems are determined by the interplay of the strong repulsion of 4f electrons on the rare-earth ion sites, their hybridization with wide-band conduction electrons and the influence of the crystalline electrical field. Consequences of the mentioned interplay for the electronic energy-band structure near the Fermi energy (E_F) were recently studied in $YbRh_2Si_2$ and $YbIr_2Si_2$ by angle-resolved photoemission and interpreted within the periodic Anderson model [1, 2]. It was found that the hybridization of 4f electrons results in a rather flat 4f band near E_F. Additionally, renormalization of the valence state leads to the formation of a heavy band that reveals strong 4f character close to E_F. Moreover, slow valence fluctuations of the Yb ion may occur between $4f^{13}$ and closed $4f^{14}$ configurations with an average valence value of about +2.9 [3]. Evidently, these observations are consistent with a metallic behavior with very heavy charge carriers having the properties of a Landau–Fermi liquid (LFL). At the same time the thermal, magnetic and transport measurements show that the heavy fermions with a well-defined Fermi surface survive only at very low temperatures, coexisting with long-range antiferromagnetic (AF) order ($T_N = 70$ mK in $YbRh_2Si_2$) which is suppressed at a magnetic quantum critical point (QCP) [4] by an external magnetic field (at $H_c = 600$ G, $T_N \to 0$ K if the c axis $\perp H$). With further increasing magnetic field at temperatures below a characteristic temperature T^*, roughly proportional to $H - H_c$, a crossover to LFL behavior is found. At temperatures above T_N and T^*, but below the single-ion Kondo temperature T_K, the properties of the discussed materials are quite unusual and display a non-Fermi-liquid (NFL) behavior. The underlying fluctuations at the QCP are discussed to be locally critical, i.e. all the low-energy degrees of freedom have an atomic length scale [4, 5]. One of the hallmarks of this local criticality is a generalized Curie–Weiss law like $\chi \propto T^{-\alpha} + \text{const}$ for the magnetic susceptibility with an exponent $\alpha < 1$ [5, 6]. This type of behavior with $\alpha = 0.75$ was found first in $CeCu_{5.9}Au_{0.1}$ [6]. The peculiarities of these properties are related to the competition between two interactions, both originating from the above-mentioned hybridization: an exchange coupling of the local moments with the broadband conduction electrons (Kondo interaction) and an induced indirect RKKY interaction between the moments. The importance of the local properties in magnetic dynamics was mainly confirmed by the discovery of a strong and rather narrow electron paramagnetic resonance (EPR) in $YbRh_2Si_2$

Table 1. Energies, wavefunctions and g factors of the Yb^{3+} ion in a tetragonal crystal field for Γ_7^t and Γ_6^t representations.

$E_{1,2}(\Gamma_7^t) = -D \pm C/\cos\varphi_c$	$E_{3,4}(\Gamma_6^t) = D \pm A/\cos\varphi_a$
$\|1\uparrow, 2\uparrow\rangle = \pm c_{1,2}\|5/2\rangle + c_{2,1}\|-3/2\rangle$ $\|1\downarrow, 2\downarrow\rangle = \mp c_{1,2}\|-5/2\rangle - c_{2,1}\|3/2\rangle$	$\|3\uparrow, 4\uparrow\rangle = \pm a_{1,2}\|-7/2\rangle + a_{2,1}\|1/2\rangle$ $\|3\downarrow, 4\downarrow\rangle = \mp a_{1,2}\|7/2\rangle - a_{2,1}\|-1/2\rangle$
$g_\parallel^{1,2}(\Gamma_7^t) = g_J(1 \pm 4\cos\varphi_c)$	$g_\parallel^{3,4}(\Gamma_6^t) = -g_J(3 \pm 4\cos\varphi_a)$
$g_\perp^{1,2}(\Gamma_7^t) = \mp 2\sqrt{3} g_J \sin\varphi_c$	$g_\perp^{3,4}(\Gamma_6^t) = -2g_J(1 \mp \cos\varphi_a)$

and $YbIr_2Si_2$ below the Kondo temperature $T_K = 25$ and 40 K, respectively (T_K revealed by specific heat data) [7–9]. This EPR signal was quite unexpected, since it was believed that the Yb^{3+} magnetic moment at $T < T_K$ should be screened by the conduction electrons and that the EPR linewidth should reach large values $\Delta H \propto k_B T_K/g\mu_B$ by approaching T_K from above. Moreover, the main features of the observed EPR signal (anisotropy of the g factor and the EPR linewidth) reflect local properties of the Yb^{3+} ion in the crystal electric field. The integrated intensity of the EPR line is proportional to the homogeneous static magnetic susceptibility. Having these experimentally confirmed local properties at hand we assume entirely local properties of the Yb^{3+} ion in the crystal electric field in order to theoretically investigate the energy spectra, g factors of the ground state and the static magnetic susceptibility of the $YbRh_2Si_2$ and $YbIr_2Si_2$ compounds.

2. Yb^{3+} ion in tetragonal crystal field

A free Yb^{3+} ion has a $4f^{13}$ configuration with one term ^2F. As the spin–orbital coupling is much stronger than the crystal field in our compounds, the total momentum $\mathbf{J}$ is a good quantum number. The spin–orbital interaction splits the ^2F term into two multiplets: $^2F_{7/2}$ with total momentum $J = 7/2$ and $^2F_{5/2}$ with $J = 5/2$. Both are separated by about 1 eV [10] and therefore we will consider only the ground multiplet $^2F_{7/2}$. The potential of the tetragonal crystal field for an ion can be written as

$$V = \alpha B_2^0 O_2^0 + \beta(B_4^0 O_4^0 + B_4^4 O_4^4) + \gamma(B_6^0 O_6^0 + B_6^4 O_6^4). \quad (1)$$

To define energy levels and wavefunctions of the Yb^{3+} ion we have to diagonalize the matrix of the operator (1) on the states of the ground multiplet $^2F_{7/2}$. In (1) B_k^q are crystal field parameters, the operators $O_k^q(\mathbf{J})$ their matrix elements and $\alpha = 2/63$, $\beta = -2/1155$, $\gamma = 4/27027$ are given in [10].

As follows from the group theory, the two-valued irreducible representation $D^{7/2}$ of the rotation group contains two two-dimensional irreducible representations Γ_7^t and Γ_6^t of the double tetragonal group $D^{7/2} = 2\Gamma_7^t + 2\Gamma_6^t$ [10]. Therefore the states of Yb^{3+} in a tetragonal field are four Kramers doublets and to diagonalize the Hamiltonian (1) we just need to diagonalize two two-dimensional matrices corresponding to the representations Γ_7^t and Γ_6^t. Hence, the crystal field splits the lower $^2F_{7/2}$ multiplet into four Kramers doublets with energies, wavefunctions and g factors as given in table 1. In this table upper and lower signs correspond to left and right indexes; $\uparrow, \downarrow$ correspond to the Kramers doublets' effective spin projection up and down, $c_1 = \cos(\varphi_c/2)$, $c_2 = \sin(\varphi_c/2)$, $a_1 = \cos(\varphi_a/2)$, $a_2 = \sin(\varphi_a/2)$, $\tan\varphi_a = \tilde{A}/A$, $\tan\varphi_c = \tilde{C}/C$, $-\pi/2 \leqslant \varphi_a, \varphi_c \leqslant \pi/2$ and $g_J = 8/7$ is the Landé g factor. We used the parameters $A, C, D, \tilde{A}, \tilde{C}$ which are defined by the crystal field parameters:

$$\begin{aligned} A &= 4B_2^0/7 + 8B_4^0/77 + 80B_6^0/143, \\ C &= 4B_2^0/21 + 40B_4^0/77 - 560B_6^0/429, \\ D &= 2B_2^0/21 - 64B_4^0/77 - 160B_6^0/429, \\ \tilde{A} &= -8\sqrt{35}B_4^4/385 + 80\sqrt{35}B_6^4/3003, \\ \tilde{C} &= -8\sqrt{3}B_4^4/77 - 80\sqrt{3}B_6^4/1287. \end{aligned} \quad (2)$$

The Zeeman energy $g_J\mu_B\mathbf{HJ}$ in the basis $|m\sigma\rangle$ ($m = 1\ldots4, \sigma = \uparrow, \downarrow$) of each doublet could be represented by

$$\mathcal{H}_{\text{Zeeman}} = g_\parallel\mu_B H_z S_z + g_\perp\mu_B(H_x S_x + H_y S_y) \quad (3)$$

where $\mathbf{H}$ is the magnetic field, $\mathbf{S}$ is the effective spin operator with $S = 1/2$, μ_B is the Bohr magneton, and $g_\parallel$ and $g_\perp$ are g factors when the field is applied parallel and perpendicular to the c axis, respectively (table 1).

As was mentioned above, the main features of the EPR signal observed in $YbRh_2Si_2$ and $YbIr_2Si_2$ reflect the local properties of the Yb^{3+} ion. The EPR signal in $YbRh_2Si_2$ and $YbIr_2Si_2$ is highly anisotropic [8, 11]. The angular dependence of g factors in these compounds is well described by

$$g = \sqrt{g_\parallel^2\cos^2\theta + g_\perp^2\sin^2\theta}, \quad (4)$$

where θ is the angle between magnetic field and crystal c-axis orientations, with $|g_\parallel| = 0.17$, $|g_\perp| = 3.56$ for $YbRh_2Si_2$ and $|g_\parallel| = 0.855$, $|g_\perp| = 3.36$ for $YbIr_2Si_2$ at $T = 5$ K. From neutron scattering experiments [12, 13] the intervals between the ground Kramers doublet and the exited energy levels amount to $\Delta_1 = 17$ meV, $\Delta_2 = 25$ meV, $\Delta_3 = 43$ meV for $YbRh_2Si_2$ and $\Delta_1 = 18$ meV, $\Delta_2 = 25$ meV, $\Delta_3 = 36$ meV for $YbIr_2Si_2$. Unfortunately, these four independent values (three energy intervals and one parameter which define $g_\parallel$ and $g_\perp$, see table 1) do not allow us to determine five crystal field parameters unambiguously.

Figure 1 represents the diagram of g factors together with the experimental points for the effective g factors of $YbRh_2Si_2$ and $YbIr_2Si_2$ (four points with different signs of $g_\parallel$ and $g_\perp$). The solid and dashed parts of the line $g_\parallel + 2g_\perp + 7g_J = 0$ in figure 1 correspond to the doublets $E_4(\Gamma_6^t)$ and $E_3(\Gamma_6^t)$, and the solid and dashed parts of the ellipse $(g_\parallel - g_J)^2/4 + g_\perp^2/3 = 4g_J^2$ correspond to the doublets $E_2(\Gamma_7^t)$ and $E_1(\Gamma_7^t)$. It is evident from the proximity to the data (symbols in figure 1) that only the doublets $E_2(\Gamma_7^t)$ and $E_4(\Gamma_6^t)$ could be considered

Table 2. Optimal theoretical g factors of the Yb^{3+} ion in $YbRh_2Si_2$ and $YbIr_2Si_2$.

Compound	Ground doublet, φ_c, φ_a	$g_\parallel$	$g_\perp$
$YbRh_2Si_2$	$E_2(\Gamma_7^t)$, $\varphi_c = \pm 1.2660$, $-\pi/2 \leqslant \varphi_a \leqslant \pi/2$	-0.229	± 3.777
	$E_4(\Gamma_6^t)$, $\varphi_a = \pm 0.8206$, $-\pi/2 \leqslant \varphi_c \leqslant \pi/2$	-0.312	-3.844
$YbIr_2Si_2$	$E_2(\Gamma_7^t)$, $\varphi_c = \pm 1.1003$, $-\pi/2 \leqslant \varphi_a \leqslant \pi/2$	-0.929	± 3.529
	$E_4(\Gamma_6^t)$, $\varphi_a = \pm 0.9952$, $-\pi/2 \leqslant \varphi_c \leqslant \pi/2$	-0.940	-3.530

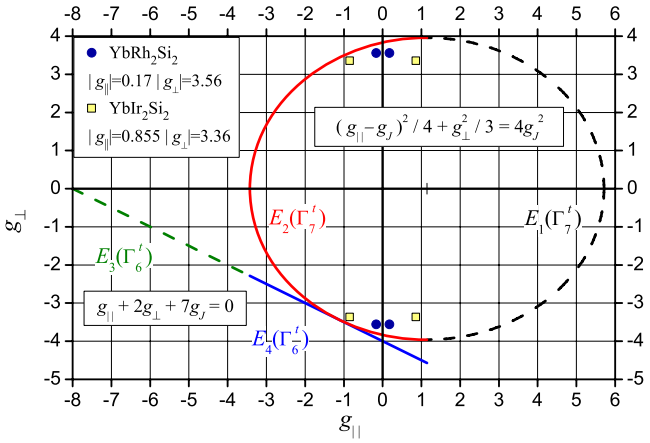

Figure 1. Diagram of g factors and experimental points at $T = 5$ K for effective g factors of $YbRh_2Si_2$ and $YbIr_2Si_2$.

for the ground state. The theoretical g values (i.e. the points on the ellipse and on the line nearest to the experimental points) and the corresponding values of φ_c and φ_a are given in table 2. These results are qualitatively well consistent with the experimental ones, being at the same time somewhat larger than the measured ones. Similar estimations for g factors were obtained recently in [14]. A slight difference between experimental and our theoretical values can be explained mainly by taking into account the above-mentioned Kondo interaction, i.e. an exchange coupling between the 4f electrons of the Yb^{3+} ion and wide-band conduction electrons. This interaction becomes highly anisotropic after projection onto the ground Kramers doublet:

$$\mathcal{H}_{\rm int} = -\sum_i \{J_{s\sigma}^{\perp}[S_i^x \sigma^x(\mathbf{r}_i) + S_i^y \sigma^y(\mathbf{r}_i)] + J_{s\sigma}^{\parallel} S_i^z \sigma^z(\mathbf{r}_i)\}. \quad (5)$$

Here $\sigma(\mathbf{r}_i)$ is the operator of the conduction electrons' spin density and $J^{\parallel,\perp}$ are the exchange coupling integrals. This leads to the so-called Knight shift of the g factor. In the case of the anisotropic exchange interaction of the antiferromagnetic sign ($J^{\parallel,\perp} < 0$) this shift reduces the absolute value of the ionic g factor in the same way as happens in the isotropic case [15, 16]:

$$g_{\parallel,\perp}^{\rm eff} = g_{\parallel,\perp}^0 (1 + \lambda_{\parallel,\perp}\chi_\sigma), \qquad \lambda_{\parallel,\perp} = \frac{J_{s\sigma}^{\parallel,\perp}}{g_{\parallel,\perp} g_\sigma \mu_{\rm B}^2} \quad (6)$$

where $g_{\parallel,\perp}^0$ is the ionic g factor, g_σ is the g factor of the conduction electrons, χ_σ is the Pauli magnetic susceptibility and $\lambda_{\parallel,\perp}$ are molecular field constants. We also have performed an improvement of this simplest contribution of the Kondo interaction by the methods of a renormalization group analysis. Then, as will be published elsewhere, critical terms like $\ln^{-1}(T/T_K^{\parallel,\perp})$ appear which reduce further the g factor values at low temperatures.

3. Static magnetic susceptibility

The magnetization of the crystal is $n\langle M\rangle$, where n is the ion concentration, $M = -g_J\mu_B\mathbf{J}$ is the ions' magnetic moment operator, $\langle M_\alpha\rangle = \mathrm{Tr}(\exp(-\beta\mathcal{H})M_\alpha)/\mathrm{Tr}\exp(-\beta\mathcal{H})$ is the mean value of the α component of the magnetic moment, $\beta = 1/(k_B T)$, k_B is the Boltzmann constant and T is the temperature. $\mathcal{H} = V - \mathbf{MH}$ is the Hamiltonian, where V is the crystal field potential (1) of the Yb^{3+} ion and the second term corresponds to the interaction of the magnetic moment with the magnetic field $\mathbf{H}$.

The magnetic susceptibility is defined as

$$\chi_{\alpha\gamma} = n\frac{\partial\langle M_\alpha\rangle}{\partial H_\gamma}\bigg|_{\mathbf{H}=0} = n\int_0^\beta \langle M_\alpha M_\gamma(\lambda)\rangle_0 \,\mathrm{d}\lambda, \quad (7)$$

where $\langle\cdots\rangle_0$ is calculated with V, $M_\alpha(\lambda) = \exp(-\lambda V)M_\alpha \exp(\lambda V)$. If we suppose the temperature to be so low that $\exp[-\beta(E_m - E_k)] \approx 0$ for $m \neq k$ we distinguish two different contributions in the susceptibility $\chi = \chi^{\rm C} + \chi^{\rm VV}$:

$$\chi_{\alpha\gamma}^{\rm C} = \frac{n\beta(g_J\mu_B)^2}{2}\sum_{\sigma\sigma'}\langle k\sigma|J_\alpha|k\sigma'\rangle\langle k\sigma'|J_\gamma|k\sigma\rangle \equiv \frac{C_{\alpha\gamma}^0}{T}, \quad (8)$$

$$\chi_{\alpha\gamma}^{\rm VV} = n(g_J\mu_B)^2 \sum_{\substack{m(\neq k)\\ \sigma\sigma'}} \frac{\langle k\sigma|J_\alpha|m\sigma'\rangle\langle m\sigma'|J_\gamma|k\sigma\rangle}{E_m - E_k}. \quad (9)$$

Here $\sigma, \sigma' = \uparrow, \downarrow$. The first term, $\chi_{\alpha\gamma}^{\rm C}$, corresponds to the Curie susceptibility proportional to the inverse temperature, while the second term, $\chi_{\alpha\gamma}^{\rm VV}$, corresponds to the Van Vleck susceptibility, which does not depend on temperature. $|k\sigma\rangle$ indicates the states of the ground Kramers doublet. In the basis of the Kramers doublet states $|m\sigma\rangle$: $\chi_{xz} = \chi_{yz} = 0$ and $\chi_{xx} = \chi_{yy} \equiv \chi_\perp$, which is the evident result for tetragonal symmetry. We also introduce $\chi_{zz} = \chi_\parallel$, and for the Curie constants $C_{zz}^0 \equiv C_\parallel^0$, $C_{xx}^0 = C_{yy}^0 \equiv C_\perp^0$.

As was shown above, the Kramers doublets $E_2(\Gamma_7^t)$ and $E_4(\Gamma_6^t)$ describe the ground state properties almost equally well. For these two cases the Curie and Van Vleck parts of the susceptibility could be expressed by the parameters c_i, a_i and energy intervals between the Kramers doublets. If the ground

Table 3. Calculated Curie constant C^0 (10^{-6} m^3 mol^{-1} K) and Van Vleck susceptibility χ^{VV} (10^{-6} m^3 mol^{-1}) for $YbRh_2Si_2$ and $YbIr_2Si_2$.

Compound	Ground doublet	$C^0_\perp$	$\chi^{VV}_\perp$	$C^0_\parallel$	$\chi^{VV}_\parallel$
$YbRh_2Si_2$	$E_2(\Gamma_7^t)$	16.8	0.087–0.202	0.062	0.09–0.227
	$E_4(\Gamma_6^t)$	17.4	0.107–0.237	0.115	0.053–0.134
$YbIr_2Si_2$	$E_2(\Gamma_7^t)$	14.7	0.121–0.215	1.02	0.094–0.187
	$E_4(\Gamma_6^t)$	14.7	0.127–0.224	1.04	0.083–0.166

state is $E_2(\Gamma_7^t)$ then

$$\chi^C_\parallel = n\beta(g_J\mu_B)^2(\tfrac{5}{2}c_2^2 - \tfrac{3}{2}c_1^2)^2,$$
$$\chi^C_\perp = 12n\beta(g_J\mu_B)^2c_1^2c_2^2,$$
$$\chi^{VV}_\parallel = \frac{32n(g_J\mu_B)^2c_1^2c_2^2}{E_1 - E_2},$$
$$\chi^{VV}_\perp = n(g_J\mu_B)^2\left[\frac{6(c_1^2 - c_2^2)^2}{E_1 - E_2} + \frac{(\sqrt{7}c_2a_1 - \sqrt{15}c_1a_2)^2}{2(E_3 - E_2)} + \frac{(\sqrt{7}c_2a_2 + \sqrt{15}c_1a_1)^2}{2(E_4 - E_2)}\right]. \quad (10)$$

If the ground state is $E_4(\Gamma_6^t)$ then

$$\chi^C_\parallel = n\beta(g_J\mu_B)^2(\tfrac{1}{2}a_1^2 - \tfrac{7}{2}a_2^2)^2, \qquad \chi^C_\perp = 4n\beta(g_J\mu_B)^2a_1^4,$$
$$\chi^{VV}_\parallel = \frac{32n(g_J\mu_B)^2a_1^2a_2^2}{E_3 - E_4},$$
$$\chi^{VV}_\perp = n(g_J\mu_B)^2\left[\frac{8a_1^2a_2^2}{E_3 - E_4} + \frac{(\sqrt{7}c_1a_2 - \sqrt{15}c_2a_1)^2}{2(E_1 - E_4)} + \frac{(\sqrt{7}c_2a_2 + \sqrt{15}c_1a_1)^2}{2(E_2 - E_4)}\right]. \quad (11)$$

The calculated molar susceptibility values are given in table 3. Here we used the g factors and parameters φ_c and φ_a from table 2. In table 3 the maximal and minimal possible values of $\chi^{VV}_{\parallel,\perp}$ for different excited doublet sequences and uncertain parameters $-\pi/2 \leqslant \varphi_a$ and $\varphi_c \leqslant \pi/2$ are given. We used for calculations experimental values of the energy intervals Δ_i. It follows from our calculations that Curie–Weiss and Van Vleck susceptibilities play different roles in parallel and perpendicular orientations: for $YbRh_2Si_2$ the Curie constant in the perpendicular orientation $C^0_\perp$ is at least two orders of magnitude larger than the Curie constant in the parallel orientation $C^0_\parallel$, whereas the Van Vleck susceptibility $\chi^{VV}_\perp$ has the same order of magnitude as $\chi^{VV}_\parallel$. For $YbIr_2Si_2$ the situation is significantly different: $C^0_\perp$ and $C^0_\parallel$ differ only by one order of magnitude whereas the Van Vleck part is almost the same as for $YbRh_2Si_2$.

4. Comparison with the experimental data

It is evident that the measured susceptibility includes both the Yb^{3+} ions and the conduction electrons' susceptibilities. In the molecular field approximation the Kondo interaction and RKKY interactions renormalize the total susceptibility [15–17]:

$$\chi_{\parallel,\perp} + \chi_\sigma = \frac{\chi^0_{\parallel,\perp} + \chi^0_\sigma + 2\lambda_{\parallel,\perp}\chi^0_{\parallel,\perp}\chi^0_\sigma}{1 - (\lambda^2_{\parallel,\perp}\chi^0_\sigma + \alpha_{\parallel,\perp})\chi^0_{\parallel,\perp}}, \qquad \chi^0_{\parallel,\perp} = \frac{C^0_{\parallel,\perp}}{T}, \quad (12)$$

where $\alpha_{\parallel,\perp}$ are additional contributions to the molecular field from the RKKY interaction [17].

This renormalization leads to a Curie–Weiss law just as in the isotropic case [15]. The Pauli susceptibility is negligible. We neglected also the renormalization of the Van Vleck part of the susceptibility. Finally, in the molecular field approximation we can write for the total magnetic susceptibility:

$$\chi^{tot}_{\parallel,\perp} = \frac{C_{\parallel,\perp}}{T + \theta_{\parallel,\perp}} + \chi^{VV}_{\parallel,\perp} \quad (13)$$

with

$$C_{\parallel,\perp} = C^0_{\parallel,\perp}(1 + 2\lambda_{\parallel,\perp}\chi^0_\sigma) \quad (14)$$

and $\theta_{\parallel,\perp}$ independent of temperature. It is evident that we should expect $C < C^0$ if $\lambda < 0$.

Figures 2 and 3 show the temperature dependence of susceptibility in $YbRh_2Si_2$ and $YbIr_2Si_2$ above 2 K. It is easy to notice that the experimental data reflect the theoretically predicted tendencies according to expression (13). Indeed, for $YbRh_2Si_2$ in perpendicular orientation the main role is played by the Curie–Weiss contribution to susceptibility, but in parallel orientation the susceptibility is almost temperature-independent and the main contribution comes from the Van Vleck part. For $YbIr_2Si_2$ the role of the Curie–Weiss susceptibility in parallel orientation is more important in comparison with $YbRh_2Si_2$.

Table 4 presents the values of the fitting parameters $C_\perp$, $\chi^{VV}_\perp$ and $C_\parallel$, $\chi^{VV}_\parallel$ for $YbRh_2Si_2$ and $YbIr_2Si_2$ (as shown in figure 2 for $YbRh_2Si_2$ $C_\parallel$ can be neglected within experimental

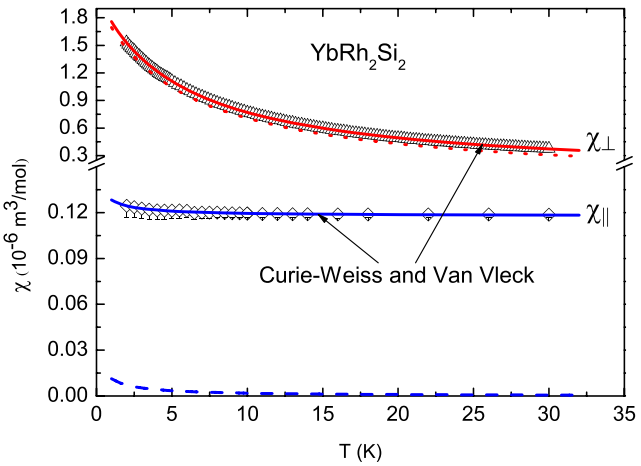

Figure 2. Static magnetic susceptibility of $YbRh_2Si_2$. Solid lines: fitting of susceptibility data with expression (13) and parameters shown in table 4. Dotted and dashed lines: contributions of the Curie–Weiss part of the susceptibility in perpendicular ($H = 11.2$ kG) and parallel orientations ($H = 10$ kG), correspondingly. Error bars indicate orientational precision. Note the different scales for $\chi_\perp$ and $\chi_\parallel$.

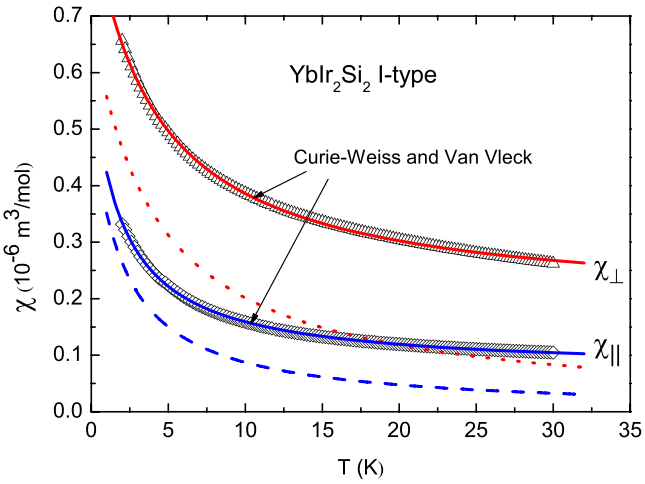

Figure 3. Static magnetic susceptibility of $YbIr_2Si_2$ for $H = 10$ kG. Solid lines: fitting of susceptibility data with expression (13) and parameters shown in table 4. Dotted and dashed lines: contributions of the Curie–Weiss part of the susceptibility in perpendicular and parallel orientations, correspondingly.

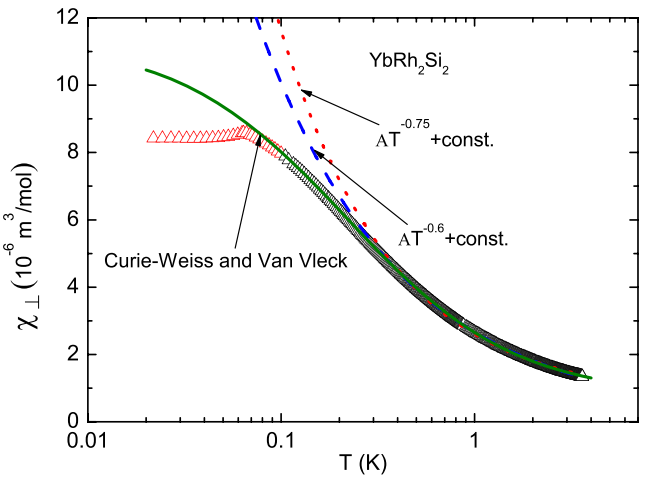

Figure 4. Fitting of the ac susceptibility data without additional dc field from [18] by the power law (15) with $\alpha = 0.6$ (dotted line), $\alpha = 0.75$ (dashed line) and by expression (13) (solid line) with parameters shown in table 4.

Table 4. Curie constants C (10^{-6} m^3 mol^{-1} K) and Van Vleck susceptibility χ^{VV} (10^{-6} m^3 mol^{-1}) for $YbRh_2Si_2$ and $YbIr_2Si_2$ from the data fits according to equation (13) as shown in figures 2–4.

Compound	T (K)	$C_\perp$	$\chi_\perp^{VV}$	$\theta_\perp$	$C_\parallel$	$\chi_\parallel^{VV}$	$\theta_\parallel$
$YbRh_2Si_2$	2–30	10.89	0.064	5.43	0.02	0.12	0.76
	0.1–3.6	2.31	0.75	0.22	—	—	—
$YbIr_2Si_2$	2–30	2.84	0.18	4.1	1.04	0.07	1.98

error). As expected, the values of parameters $C_\perp$ and $C_\parallel$ are smaller than the calculated values $C_\perp^0$ and $C_\parallel^0$. Indeed, as follows from (13), the renormalization of the susceptibility by the interaction with conduction electrons reduces the value of Curie constants because of the antiferromagnetic sign of the exchange integral ($J^{\parallel,\perp} < 0$) and, hence, $\lambda_{\parallel,\perp} < 0$. From our fitting the Weiss temperatures are $\theta_\perp = 5.43$ K, $\theta_\parallel = 0.76$ K for $YbRh_2Si_2$ and $\theta_\perp = 4.1$ K, $\theta_\parallel = 1.98$ K for $YbIr_2Si_2$.

5. Discussion

Our calculations of the magnetic susceptibility of $YbRh_2Si_2$ and $YbIr_2Si_2$ on the basis of an entirely local model of the Yb^{3+} ion in the crystal electric field were stimulated for the following reasons. Firstly, the observed EPR signal reflects a number of features, which are very similar to those expected for Yb^{3+} ions doped in non-conducting crystals (in particular, the local crystal field symmetry, the value of g factors and the temperature dependence of the EPR intensity, see [10]). Even the EPR linewidth shows a temperature dependence that resembles the behavior of Yb^{3+} ions diluted in a conducting environment [7, 15]. Secondly, an intensive experimental study of the NFL magnetic and thermal properties of these materials points out locally critical fluctuations. Thirdly, the calculations for the local model used could be performed in a straightforward and transparent way.

Our major result is a remarkable agreement of our local approach for the static magnetic susceptibility with the temperature dependence of the experimental data. Therefore, in the considered region of temperatures (0.1–30 K) a ballistic motion of the 4f electrons is practically absent, and they could be considered as quasi-localized. However, when approaching lower temperatures, ferromagnetic quantum critical fluctuations dominate [4, 18] and a locally quantum critical scenario may be applicable [5]. One of the hallmarks of this scenario is a generalized Curie–Weiss law which, for a wavevector-dependent magnetic susceptibility, can be written in the form

$$\chi(\mathbf{q}, T) = \frac{C}{T^\alpha + \theta(\mathbf{q})^\alpha} \tag{15}$$

with an exponent $\alpha < 1$ [5, 6]. In the case of $YbRh_2Si_2$ such a behavior was revealed in the temperature region 0.3 K $< T <$ 10 K for $\mathbf{q} = 0$, with $\alpha = 0.6$ and $\theta = 0$ [18]. As shown in figure 4, we point out that a Curie–Weiss law together with a Van Vleck contribution convincingly describes the data for a wider temperature region in comparison with equation (15) and down to temperatures just above the AFM ordering temperature. However, for the temperature region shown in figure 4 the fitting parameters for the low temperature region are considerably changed, see table 4. The reduction of the Curie constant C and Weiss temperature ($\theta = 0.22$ K), as well as an increase of the temperature-independent contribution, can be related to the approach of the system to the LFL regime with a more ballistic motion of the 4f electrons and indicate the Kondo effect in the magnetic susceptibility data. In this respect a Curie–Weiss description well within the Kondo regime, i.e. at $T \ll T_K$, despite being successful, may appear to be not appropriate. However, strong ferromagnetic correlations, as indicated, for instance, by a large Sommerfeld–Wilson ratio for $YbRh_2Si_2$ [18] and $YbIr_2Si_2$ [9], dominate the magnetic susceptibility and may lead to this Curie–Weiss behavior. The reduction of the Curie constant can also be observed experimentally when comparing

the magnetic susceptibility per Yb ion of $YbRh_2Si_2$ with $Y_{1-x}Yb_xPd_3$ ($x = 0.6\%$) where the 4f electrons are not hybridized with the conduction electrons [19]. Interestingly, the Yb^{3+} EPR intensity of the YPd_3:Yb system compares well with the EPR intensity of $YbRh_2Si_2$ [19]. In respect to this yet unexplained observation, it is worth mentioning that, in spite of the success of our entirely local approach for the static magnetic susceptibility of $YbRh_2Si_2$, this model is insufficient for a proper theoretical understanding of the dynamical susceptibilities as observed by EPR. We have found that this problem can be considered by taking into account a translational diffusion of 4f electrons and their collective response together with wide-band conduction electrons to the resonant magnetic alternating field (the bottleneck regime). However, a discussion of this problem is beyond the scope of this paper and results will be published elsewhere.

Acknowledgments

This work was supported by the Volkswagen Foundation (I/82203) and partially by the RF President Program 'Leading scientific schools' 2808.2002.2; AMS was supported partially by cooperative grant Y4-P-07-15 from the CRDF BRHE Program and from the RF Ministry of Education and Science, RNP. 2.2.2.3.10028.

References

[1] Danzenbächer S *et al* 2007 *Phys. Rev.* B **75** 045109
[2] Vyalikh D V *et al* 2008 *Phys. Rev. Lett.* **100** 056402
[3] Knebel G *et al* 2006 *J. Phys. Soc. Japan* **75** 114709
[4] Gegenwart P, Si Q and Steglich F 2008 *Nat. Phys.* **4** 186
[5] Si Q, Rabello S, Ingersent K and Smith L 2001 *Nature* **413** 804
[6] Schröder A, Aeppli G, Coldea R, Adams M, Stockert O, von Löhneysen H, Bucher E, Ramazashvili R and Coleman P 2000 *Nature* **407** 351
[7] Sichelschmidt J, Ivanshin V A, Ferstl J, Geibel C and Steglich F 2003 *Phys. Rev. Lett.* **91** 156401
[8] Sichelschmidt J, Wykhoff J, Krug von Nidda H-A, Fazlishanov I I, Hossain Z, Krellner C, Geibel C and Steglich F 2007 *J. Phys.: Condens. Matter* **19** 016211
[9] Hossain Z, Geibel C, Weickert F, Radu T, Tokiwa Y, Jeevan H, Gegenwart P and Steglich F 2005 *Phys. Rev.* B **72** 094411
[10] Abragam A and Bleaney B 1970 *Electron Paramagnetic Resonance of Transition Ions* (Oxford: Clarendon)
[11] Sichelschmidt J, Wykhoff J, Krug von Nidda H-A, Ferstl J, Geibel C and Steglich F 2007 *J. Phys.: Condens. Matter* **19** 116204
[12] Stockert O, Koza M M, Ferstl J, Murani A P, Geibel C and Steglich F 2006 *Physica* B **378–380** 157–8
[13] Hiess A, Stockert O, Koza M M, Hossain Z and Geibel C 2006 *Physica* B **378–380** 748–9
[14] Leushin A M, Ivanshin V A and Kurkin I N 2007 *Phys. Solid State* **49** 1417–21
[15] Barnes S E 1981 *Adv. Phys.* **30** 801–938
[16] Kochelaev B I and Safina A M 2004 *Phys. Solid State* **46** 226–30
[17] Mattis D C 1965 *The Theory of Magnetism* (New York: Harper and Row)
[18] Gegenwart P, Tokiwa Y, Custers J, Geibel C and Steglich F 2006 *J. Phys. Soc. Japan* **75** (Suppl.) 155
[19] Wykhoff J, Sichelschmidt J, Lapertot G, Knebel G, Flouquet J, Fazlishanov I I, Krug von Nidda H-A, Krellner C, Geibel C and Steglich F 2007 *Sci. Tech. Adv. Mater.* **8** 389